Assessing aerosol induced errors in Monte Carlo based air-shower reconstruction for atmospheric Cherenkov detectors

Assessing aerosol induced errors in Monte Carlo based air-shower reconstruction for atmospheric Cherenkov detectors

T L Holch[1], F Leuschner[2], J Schäfer[3] and S Steinmassl[4]

[1]Deutsches Elektronen-Synchrotron DESY, Platanenallee 6, 15738 Zeuthen, Germany
[2]Institut für Astronomie und Astrophysik, Universität Tübingen, Sand 1, D 72076 Tübingen, Germany
[3]Friedrich-Alexander-Universität Erlangen-Nürnberg, Erlangen Centre for Astroparticle Physics, Erwin-Rommel-Str. 1, D 91058 Erlangen, Germany
[4]Max-Planck-Institut für Kernphysik, P.O. Box 103980, D 69029 Heidelberg, Germany

E-mail: tim.lukas.holch@desy.de

Abstract. Aerosol levels influence the wavelength dependent transmission properties of the atmosphere. Variations in aerosol levels therefore affect the amount of Cherenkov light from air-showers that can reach an atmospheric Cherenkov detector. As the amount of detected Cherenkov light is directly related to a primary shower particle's energy, deviations between actual and assumed atmospheric transmission properties yield errors in reconstructed particle energies as well as energy axes of instrument response functions. In this work, a scheme is presented to assess this influence and potentially reduce related errors in the air-shower reconstruction. The proposed scheme relies on estimations or measurements of the aerosol optical depth and atmospheric density profile which are then used in radiative transfer simulations to generate atmospheric transmission profiles. As the scheme furthermore uses detector specific quantum efficiencies and generalised shower evolution models, it does not rely on detailed Monte Carlo simulations for the different atmospheric conditions but only on the transmission profile which the initial shower reconstruction algorithm is based on. The approach is derived and presented on the example of the H.E.S.S. experiment which employs imaging atmospheric Cherenkov telescopes in the Khomas Highland of Namibia to detect gamma rays in the GeV to TeV energy range.

1. Introduction

As the atmosphere serves as calorimeter for atmospheric Cherenkov detectors, a good knowledge of the atmospheric conditions during a measurement is important to correctly interpret the collected data. The atmosphere is however a highly variable system with optical properties that depend on a multitude of parameters that are near impossible to monitor constantly. In common air-shower reconstruction algorithms, measured signals are compared to extensive Monte Carlo (MC) simulations of the detector response to showers under certain conditions. In order to analyse data taken with atmospheric Cherenkov detectors, it is therefore necessary to make certain assumptions about the atmospheric conditions at the time of a measurement. A difference between assumed and actual atmospheric conditions can thereby cause a systematic misreconstruction of air-shower parameters, in particular an over- or underestimation of shower

energies, which also affects the accuracy of the assumed instrument response functions (IRFs) and thereby also reconstructed particle fluxes. Among all atmospheric parameters, aerosols have been shown to have a particularly significant impact on the propagation of Cherenkov light in the atmosphere and thus have been subject to several studies in the past [1, 2, 3] with multiple approaches being presented to account and/or correct for their influence [4, 5, 6, 7].

In this contribution, a general scheme is proposed to assess the influence of specific variations in atmospheric aerosols. It is presented on the example of the High Energy Stereoscopic System (H.E.S.S.), an experiment to detect γ-ray induced air-showers in the GeV to TeV energy range, that is seasonally impacted by significantly elevated aerosol levels (sometimes also referred to as the "*Thomas Lohse Effect*").

2. The H.E.S.S. experiment and seasonal aerosol variations

The H.E.S.S. experiment is an array of five imaging atmospheric Cherenkov telescopes (IACTs) in the Khomas Highland of Namibia [8], a region in which the annual biomass-burning season causes highly varying aerosol levels from around August to October [9]. Since 2016, a station of the Aerosol Robotic Network (AERONET) [10] is operating on the H.E.S.S. site. AERONET is a project that hosts a network of ground-based photometers distributed around the globe that provides atmospheric aerosol data which is made publicly available. Among other parameters the station at the H.E.S.S. site measures the aerosol optical depth (AOD) at several wavelengths between 340 nm and 1640 nm by tracking the Sun during the day and the Moon in nights from waxing to waning gibbous phase. AERONET furthermore provides data inversion products that include the aerosol size distribution as well as refractive index which can be used to characterise the aerosol composition.

In the data from the AERONET station at the H.E.S.S. site, the annual biomass-burning season is clearly visible as shown in Fig. 1. A change in aerosol composition during this season can also be seen in the deduced aerosol particle size distributions shown in Fig. 2.

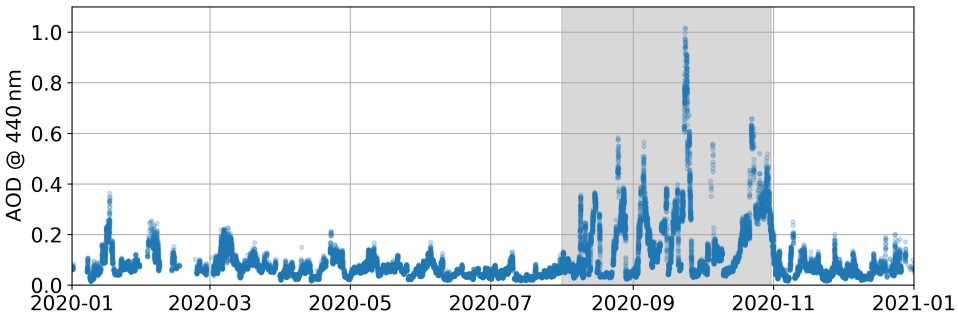

Figure 1. AOD at 440 nm measured by the AERONET station at the H.E.S.S. site for the full year 2020 (combined Sun and Moon mode in data level 1.5). The annual biomass-burning season from August to October (marked in grey) is clearly visible with AOD levels rising up to a factor of ~ 5 compared to common variations throughout the rest of the year.

3. Atmosphere description in MC simulations

MC simulations for atmospheric Cherenkov detectors usually consist of two parts. First, the interactions of shower particles in the atmosphere are simulated together with the production and propagation of Cherenkov photons. A common software for this, which is also used in H.E.S.S. data analyses, is the CORSIKA package [11]. In the second step, the detector response is simulated, which includes the optical setup as well as the electronics and readout, which can e.g. be done with the sim_telarray package [12]. The atmospheric conditions are thereby described

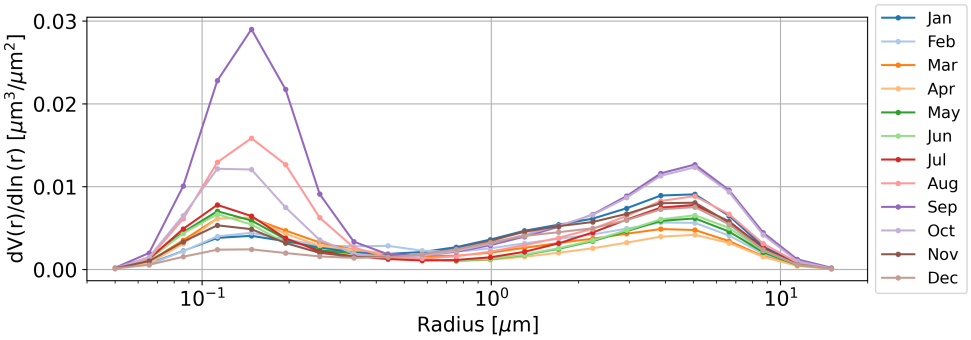

Figure 2. Monthly mean aerosol size distributions for the H.E.S.S. site in 2020 from AERONET inversion products. The months of the biomass-burning season show clearly elevated levels in low-radii aerosol particles compared to the other months of the year.

by a density profile and a transmission profile. The density profile includes parameters such as air pressure, density and refractive index over the full altitude profile and mainly influences the evolution and propagation of shower particles. The transmission profile provides the transmission probability for radiation of a given wavelength to travel from a certain altitude down to the detector level and depends on various atmospheric parameters ranging from temperature and humidity to gaseous content and aerosols. To generate transmission profiles, radiative transfer simulations have to be performed for the desired wavelengths and altitudes under the assumed atmospheric conditions as outlined further in Sec. 4.1.

4. A general scheme to assess the influence of aerosol variations

The main idea of the proposed scheme is to evaluate how much more or less Cherenkov radiation is expected for a shower of certain energy observed under specifically different aerosol conditions than the ones assumed in the MC-based shower reconstruction. This is done by comparing the transmission profile used for the MC simulations with transmission profiles of different aerosol concentrations and/or compositions. In the following, the individual steps of the scheme are outlined in detail. It is important to note that the proposed scheme assumes a linear relationship between the number of detected Cherenkov photons and the primary shower particle's energy. Furthermore, it assumes that the transmission profile only influences the total number of Cherenkov photons and not the brightness distribution.

4.1. Generating atmospheric transmission profiles

In the first step, atmospheric transmission profiles are generated by performing radiative transfer simulations for the assumed conditions using the Python interface Py6S [13] for the simulation software 6SV1, a vector version of 6S[1] [14]. Important input parameters are the atmospheric profiles for pressure, temperature, water and ozone content. For pressure, temperature and water, the overall mean profiles were calculated from the two closest stations[2] found in the Integrated Global Radiosonde Archive (IGRA) [15]. To generate an accurate ozone profile, data from IAGOS [16, 17] was used in combination with the tropical ozone model provided in 6SV1. As the variations in aerosol levels at the H.E.S.S. site are dominated by the strong increases during the biomass-burning season, the biomass-burning aerosol profile provided in 6SV1 is used. The aerosol profile can thereby be scaled by providing the AOD at 550 nm (AOD_{550}) which is used to calculate a visibility parameter. As AERONET does not measure AOD_{550}, the value

[1] 6S stands for *Second Simulation of the Satellite Signal in the Solar Spectrum*
[2] Station identifiers `WAM00068110` and `WAM00068112`

is determined via interpolation between the measurements at other wavelengths. To cover the conditions observed at the H.E.S.S. site, transmission profiles are generated for the range of AOD_{550} values deduced from the AERONET dataset, i.e. from almost 0 to ~ 1.2. Examples of the resulting transmission profiles are shown in Fig. 3.

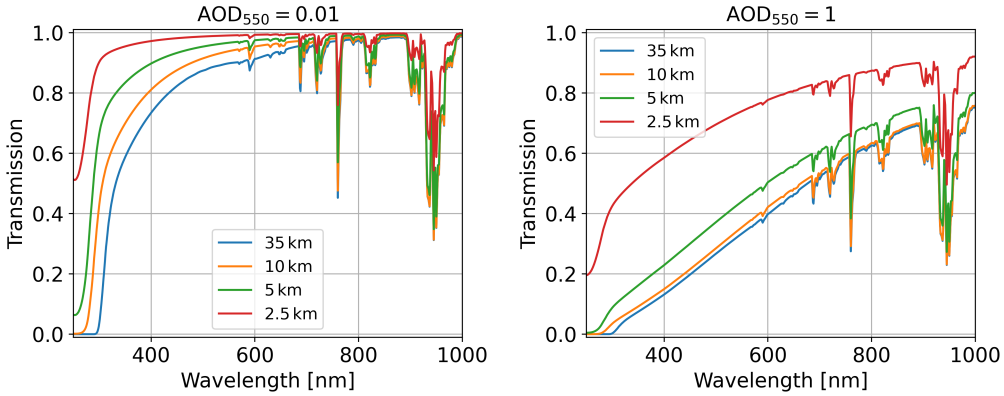

Figure 3. Examples of transmission curves generated with a biomass-burning aerosol profile scaled with an AOD_{550} of 0.01 (*left*, very low aerosol content) and 1.0 (*right*, very high aerosol content).

4.2. Calculating photon ratios

In order to estimate by what factor a MC-based shower reconstruction is off for a given aerosol condition, the generated transmission profiles T are first folded with a generic Cherenkov emission spectrum S and the wavelength dependent quantum efficiency Q of the detector before integrating over the wavelength λ. The same is then done for the MC reference T_{MC}. In the next step the one is divided by the other to obtain the photon ratio, which depends on the AOD_{550} and altitude h:

$$R(\mathrm{AOD}_{550}, h) = \frac{\int_{\lambda_{\min}}^{\lambda_{\max}} T(\mathrm{AOD}_{550}, h, \lambda) * S(\lambda) * Q(\lambda)\ d\lambda}{\int_{\lambda_{\min}}^{\lambda_{\max}} T_{\mathrm{MC}}(h, \lambda) * S(\lambda) * Q(\lambda)\ d\lambda}\ . \tag{1}$$

This ratio states how much more or less Cherenkov radiation is expected to be detected for a given aerosol condition from a given altitude compared to the MC reference. The process is visually explained in Fig. 4.

Practically, the transmission profiles are tensors (or rather tables) with discrete values in λ and h. By choosing the same discrete steps in λ for S and Q, the folding and integrating reduces to simple multiplication and summation along tensor axes.

4.3. Introducing shower energy and zenith dependency

By converting the altitude axis h of the photon ratio R to units of radiation length X_0 (which is $\sim 37\,\mathrm{g\,cm^{-2}}$ in air) via the atmospheric density profile, it is possible to fold in energy dependent parametric longitudinal γ-ray shower profiles as e.g. determined in [18]. As only the ratio to the MC reference is of interest, the profiles can be normalised to their respective maximum, yielding $N(E, X_0)$ as shown in Fig. 5 (*centre*). This introduces an energy dependency, which is significant as higher energy showers penetrate deeper into the atmosphere, meaning that Cherenkov photons from the lower end of a high energy air-shower travel through less atmosphere compared to a lower energy shower. Furthermore, by assuming a plane parallel atmosphere — i.e., by scaling

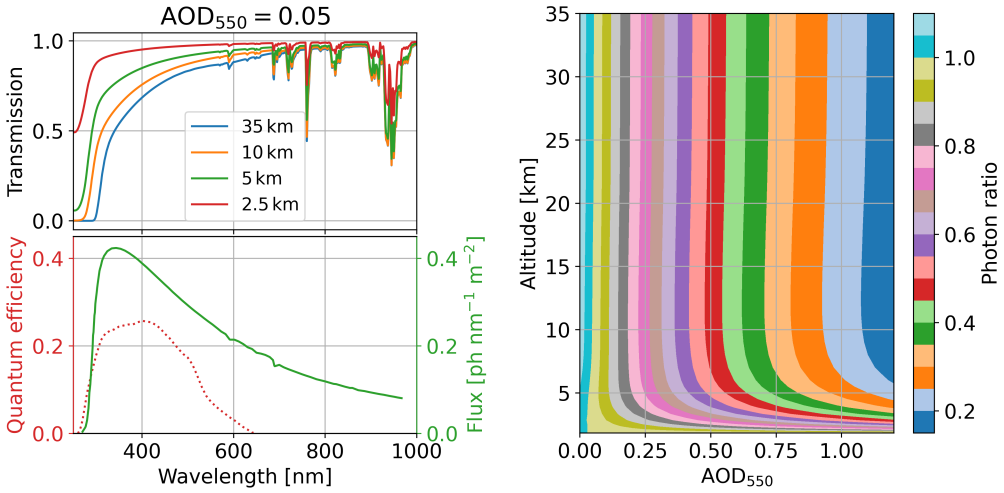

Figure 4. In order to calculate a photon ratio table R (*right*), which states the ratio of Cherenkov photons expected to be detected at ground-level for a given AOD$_{550}$ compared to a MC reference, the transmission curves (examples shown *top left*) are folded with a generic Cherenkov spectrum and the detector's quantum efficiency (*bottom left*). The results are then integrated over wavelength for each altitude and divided by the respective MC reference value.

the altitude/radiation length axis by $1/\cos(\vartheta)$ — a dependency on the zenith angle ϑ under which a shower is observed can be introduced, yielding the adapted photon ratio

$$\tilde{R}(\mathrm{AOD}_{550}, X_0, E, \vartheta) = R(\mathrm{AOD}_{550}, X_0/\cos(\vartheta)) * N(E, X_0) \ . \tag{2}$$

The procedure is shown on an example in Fig. 5 with the individual steps outlined in the caption.

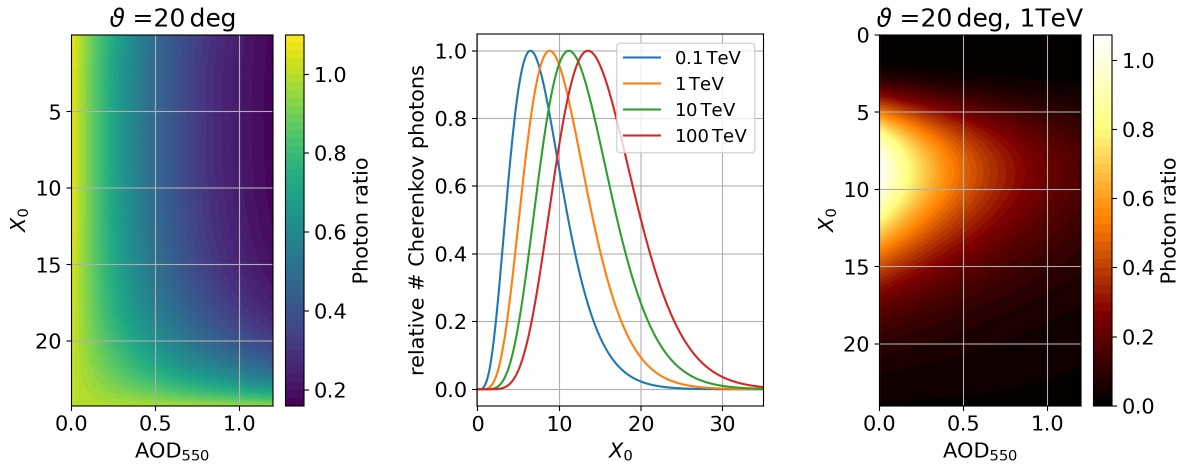

Figure 5. *Left*: By converting the altitude axis to units of radiation lengths X_0 and assuming a plane parallel atmosphere, the ratio table shown in Fig. 4 (*right*) can be converted to the shown form. By then folding in normalised longitudinal γ-ray induced air-shower profiles as shown in the *centre*, energy dependent ratio tables as shown on the *right* are generated.

4.4. Assessing systematic uncertainties

By dividing the integral along X_0 of the adapted ratio tables $\tilde{R}$ (as shown in Fig. 5 (*right*) for a 1 TeV γ-ray shower at 20 deg zenith angle) by the integral along X_0 of the respective normalised longitudinal shower profiles (as shown in Fig. 5 (*centre*)) for all zenith angles ϑ and shower energies E, a ratio factor can be deduced:

$$f_r(\mathrm{AOD}_{550}, E, \vartheta) = \frac{\int_0^{X_0^{\max}(\vartheta)} \tilde{R}(\mathrm{AOD}_{550}, X_0, E, \vartheta)\ dX_0}{\int_0^{X_0^{\max}(\vartheta)} N(E, X_0)\ dX_0}\ . \tag{3}$$

The upper bound of the integrals $X_0^{\max}$ is thereby ϑ-dependent and corresponds to the total number of radiation lengths from the top of the atmosphere down to the ground-level. The evaluation of this function provides a factor that indicates what fraction of Cherenkov radiation is expected for a shower of given energy observed under a specific AOD_{550} and zenith angle as compared to the MC reference. Fig. 6 shows the resulting values for $\vartheta = 20$ deg.

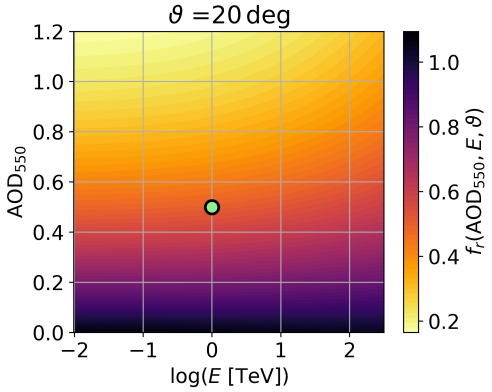

Figure 6. Ratio factor values for a zenith angle of $\vartheta = 20$ deg. The light green marker shows the position for a 1 TeV air shower observed under an AOD_{550} of 0.5.

In Fig. 6, it can be seen that e.g. from a 1 TeV air-shower observed at an AOD_{550} of 0.5 (light green marker) only around half of the Cherenkov radiation is detected as expected under MC conditions. Assuming a linear relationship between the amount of detected Cherenkov radiation and shower energy, this 1 TeV shower is therefore *reconstructed* with an energy E_r of rather ~ 0.5 TeV. To better assess the effect of different aerosol levels, the inverse of the ratio factor can be plotted for specific values of AOD_{550} and ϑ over energy, which shows how far off the MC-based energy reconstruction is under given conditions. Examples are shown in Fig. 7. As for the example above, it can be seen here that for a 1 TeV air-shower observed at an AOD_{550} of 0.5 under a zenith angle of 20 deg (light green marker on the dashed red line), the reconstructed energy will be wrong by a factor of ~ 2. The plot furthermore shows the significant energy dependency of the systematic underestimation of shower energies for higher aerosol levels and low zenith angles. For higher zenith angles and lower aerosol levels, the systematic bias is almost constant with energy. For very low aerosol concentrations, the MC-based reconstruction even overestimates shower energies as depicted by the inverse ratio < 1.

4.5. Extension to other parameters

The proposed scheme can be extended to assess the influence of various atmospheric parameters by generating according transmission profiles with Py6S, e.g., for seasonal variations in ozone or water profiles determined via IAGOS and/or IGRA data. The ratio function f_r is thereby

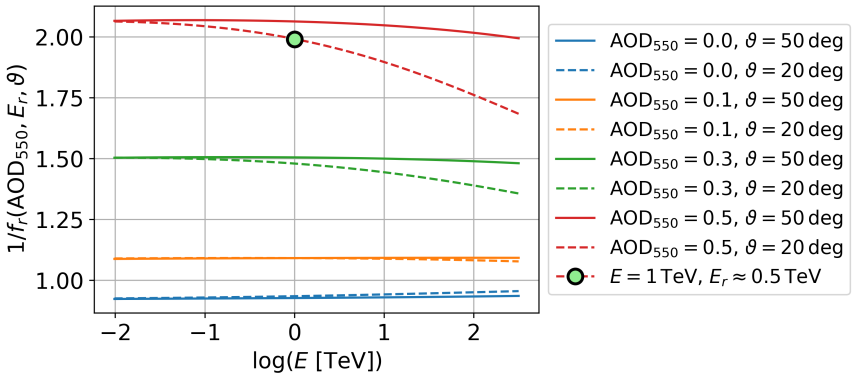

Figure 7. Inverse ratio factors for different zenith angles and aerosol levels plotted over shower energy. The light green marker on the dashed red line depicts the example from the text of a 1 TeV air shower observed at an AOD_{550} of 0.5 at 20 deg zenith.

extended to additional dimensions. Furthermore, the impact of variations in aerosol composition can be evaluated. This can e.g. be done by using the AERONET inversion products, as Py6S provides the functionality to directly use photometer data.

4.6. Application as a correction scheme

Besides assessing systematic uncertainties, the inverse of the proposed ratio factor $f_r(\mathrm{AOD}_{550}, E, \vartheta)$ can also be used to correct reconstructed air-shower energies in analyses of, e.g., IACT data. This however involves a further step, as only the reconstructed energy E_r of air showers is known in practice. In order to generate a respective correction factor, the energy dependency of f_r has to be transferred to an E_r dependency. Folding the energy axis E with the ratio function f_r thereby yields these reconstructed energies $E_r = E * f_r(\mathrm{AOD}_{550}, E, \vartheta)$. By doing this for all sets of AOD_{550} and ϑ values and performing a multi-dimensional grid interpolation on the shifted f_r, an according correction function $f_c(\mathrm{AOD}_{550}, E_r, \vartheta)$ can be generated. When correcting shower energies, it is however important to also adjust the IRFs accordingly, as also outlined in [4]. For the proposed correction scheme, the bin edges of the true energy axes of the IRFs can be multiplied with the corresponding correction factor, effectively moving and stretching/compressing the IRFs along this axis. For the application as a correction scheme, an important aspect is of course the determination of the AOD at the time of observations, which are often conducted during complete darkness. One option is a data-driven approach in which the AOD is estimated from Cherenkov detector specific parameters like the Cherenkov transparency coefficient proposed in [3]. Besides using lidar measurements, another promising alternative approach to obtain the AOD during darkness is wide-field stellar photometry as presented in [19].

5. Conclusions

In this contribution, a general scheme to assess systematic errors in MC-based air-shower reconstructions caused by atmospheric variations is presented on the example of the H.E.S.S. experiment, which is strongly impacted by the annual biomass-burning season in southern Africa. In the presented example, a certain transmission profile is assumed to be used in a MC-based air-shower reconstruction. This profile is then compared to transmission profiles generated via radiative transfer simulations for different aerosol conditions on the basis of AOD measurements by the AERONET station on the H.E.S.S. site. The scheme is then used to assess the expected systematic errors on reconstructed γ-ray energies. Besides investigating aerosol-

induced uncertainties, the scheme can be adapted to assess the influence of various atmospheric parameters by generating the according transmission profiles and following the steps of the proposed scheme. Its application can furthermore be extended to correct for atmosphere induced errors in reconstructed air-shower energies. This is currently explored within the H.E.S.S. collaboration and will be the subject of a forthcoming publication.

Acknowledgments

The authors thank the members of the H.E.S.S. collaboration for supporting this project and providing valuable feedback. The authors furthermore thank the AERONET project and in particular Nichola Knox as the principal investigator for their effort in establishing and maintaining the HESS AERONET site.

MOZAIC/CARIBIC/IAGOS data were created with support from the European Commission, national agencies in Germany (BMBF), France (MESR), and the UK (NERC), and the IAGOS member institutions (http://www.iagos.org/partners). The participating airlines (Lufthansa, Air France, Austrian, China Airlines, Hawaiian Airlines, Iberia, Cathay Pacific, Air Namibia, Sabena) supported IAGOS by carrying the measurement equipment free of charge since 1994. The data are available at http://www.iagos.fr thanks to additional support from AERIS.

References

[1] Bernlöhr K 2000 *Astroparticle Physics* **12** 255–268 ISSN 0927-6505 URL https://www.sciencedirect.com/science/article/pii/S0927650599000936
[2] Abraham J, Abreu P, Aglietta M *et al.* 2010 *Astroparticle Physics* **33** 108–129 ISSN 0927-6505 URL https://www.sciencedirect.com/science/article/pii/S0927650509001935
[3] Hahn J, de los Reyes R, Bernlöhr K *et al.* 2014 *Astroparticle Physics* **54** 25–32 ISSN 0927-6505 URL https://www.sciencedirect.com/science/article/pii/S0927650513001540
[4] Fruck, Christian and Gaug, Markus 2015 *EPJ Web of Conferences* **89** 02003 URL https://doi.org/10.1051/epjconf/20158902003
[5] Dawson, Bruce R 2019 *EPJ Web Conf.* **197** 01004 URL https://doi.org/10.1051/epjconf/201919701004
[6] Devin J, Bregeon J, Vasileiadis G and Gallant Y 2019 *EPJ Web Conf.* **197** 01001 URL https://doi.org/10.1051/epjconf/201919701001
[7] Holler M, Lenain J P, de Naurois M *et al.* 2020 *Astroparticle Physics* **123** 102491 ISSN 0927-6505 URL https://www.sciencedirect.com/science/article/pii/S0927650520300633
[8] H.E.S.S. homepage: URL https://www.mpi-hd.mpg.de/hfm/HESS/
[9] Formenti P, D'Anna B, Flamant C *et al.* 2019 *Bulletin of the American Meteorological Society* **100** 1277 – 1298 URL https://journals.ametsoc.org/view/journals/bams/100/7/bams-d-17-0278.1.xml
[10] Holben B, Eck T, Slutsker I *et al.* 1998 *Remote Sensing of Environment* **66** 1–16 ISSN 0034-4257 URL https://www.sciencedirect.com/science/article/pii/S0034425798000315
[11] Heck D, Knapp J, Capdevielle J *et al.* 1998 CORSIKA: A Monte Carlo code to simulate extensive air showers Tech. Rep. FZKA-6019
[12] Bernlöher K 2008 *Astroparticle Physics* **30** 149 – 158 ISSN 0927-6505 URL http://www.sciencedirect.com/science/article/pii/S0927650508000972
[13] Wilson R 2013 *Computers & Geosciences* **51** 166–171 ISSN 0098-3004 URL https://www.sciencedirect.com/science/article/pii/S0098300412002798
[14] Vermote E, Tanre D, Deuze J *et al.* 1997 *IEEE Transactions on Geoscience and Remote Sensing* **35** 675–686
[15] Durre I, Yin X, Vose R S *et al.* 2018 *Journal of Atmospheric and Oceanic Technology* **35** 1753 – 1770 URL https://journals.ametsoc.org/view/journals/atot/35/9/jtech-d-17-0223.1.xml
[16] Clark H L 2020 *IOP Conference Series: Earth and Environmental Science* **509** 012008 URL https://doi.org/10.1088/1755-1315/509/1/012008
[17] IAGOS data profiles: URL https://doi.org/10.25326/07
[18] Sajjad S and Falvard A 2020 A parameterisation of the longitudinal cherenkov emission profiles of gamma induced electromagnetic showers in the atmosphere in the gev-tev energy range URL https://arxiv.org/abs/2010.13822
[19] Ebr J, Karpov S, Eliášek J *et al.* 2021 *The Astronomical Journal* **162** 6 URL https://doi.org/10.3847/1538-3881/abf7b1